Extraction and update of area water bodies from remote sensing imagery using vector data and snake models under similarity restriction

AN Xiaoya **, YANG Yun**

* State Key Laboratory of Geographical Information Engineering, Xi' an 710054，China
** Xi,an Research Institute of Surveying and Mapping , Xi' an 710054，China

Abstract. As the initial location of the vector data, this paper presents a new active contour model, which is used to extract area water bodies from remote sensing images. The new active contour model is added to the image gravitation potential energy based on object-background gray values, as well as to the similarity restriction potential energy based on discrete curvature. The purpose of the new model is to improve the constringency speed and noise immunity of the existing model, and to avoid noise from occurring on the curve point of attraction and disturbance. The new model makes thorough use of prior information obtained from vector data, in order to adaptively compute the correlative parameters. In addition, the extraction precision evaluating model is established based on similarity measurement, and the model solving process is determined based on the greedy algorithm. Finally, experiments are performed to show the feasibility and superiority of the method.

Keywords: spatial data updating, contour extraction, active contour model, similarity restriction, prior information

1. Introduction

Both the focus and most difficult point of this study is the automatic extraction of geographic information from remote sensing images (those

involved in this study being visible images), so as to continuously update vector data. One of the main directions of study in this field is to extract geographic information using an active contour model for example: SALMAN (2010), Matthias (2004, 2007, and 2010), HU (2009), Miao (2010). The concept of the active contour model was first presented by Kass in 1987 Kass (1987); its main advantage is that it integrates image data, initial estimation, target contour characteristics and knowledge-based restriction conditions into a single characteristic extraction process, which is performed during model evolution. However, the largest setbacks of the traditional active contour model are that it is very sensitive to initial location CHEN (2007), and that it is not able to easily obtain the initial location; at the same time, the vector data may be regarded as the initial location of the active contour model, and may provide a large amount of priori knowledge during the data updating process. Therefore, one common method used by researchers is to apply vector data as previously existing knowledge in image contour edge extraction HaN (2009) and the integrated update model based on images and vector data has been preliminarily applied in large-scale engineering practices CHEN (2010). For instance, HaN (2009) presented an automatic GIS vector boundary update method based on the grouping snake model; Zhang(2007) and Stefan(2008) detected and extracted change information of water systems with the active contour model based on images and vector data; and Matthias(2007) integrated raster and vector data with the traditional snake model.

The main disadvantages of the above methods are as follows: The noise immunity of the model is poor, and the contour control points may easily converge to local extreme points, due to the attraction and disturbance originating from noise points, causing the finally extracted area water body to vary greatly from the actual contour. The initial vector and image data possess different currencies, and differences also exist in their spatial locations, shapes, areas and other characteristics; however, due to the fact that they express the same ground object entity (such as a water body), they are greatly similar to each other in terms of shape. Consequently, in order to retain the similarity between the geometrical shape of the object and the contour shape of the vector data, this paper adds similarity potential energy to the model so as to extract correct water body information.

In addition, traditional models only use gradient intensity to construct external forces. If the gradient force is a short-range force and the vector data are located at a significant distance from the object's edges, this short-range force may not be able to "pull" the vector contour to the true edges, thus causing the convergence speed to become slow. Therefore, this paper designs a long-range image gravitation based on the object-background gray value, in order to improve the convergence speed; as the adaptive

ability and automation degree of traditional models are both quite poor, References SALMAN (2010) and HU (2009) applied prior information which had been obtained manually. The paper makes thorough use of the prior vector data information, and attempts to compute parameters adaptively in the model realization process, so as to enhance the automation degree.

2. Traditional active contour model

The active contour model means movable curves defined in the image domain and their movements are controlled by their own internal force as well as the external force from the image data. The internal force restrains the shapes of the curves and retains curve smoothness and continuity, and the external force leads the contour curves to evolve toward the target characteristics. Finally, the total energy of the curves reaches the minimum level under the combined balancing effects of the external and internal forces, and the contour information of the object may be extracted. The mathematical expression of the active contour model is expressed with parameters. Supposing $\boldsymbol{v}(s) = [x(s), y(s)]$, $s \in [0,1]$ where s represents the arc length of the normalized curve, the energy function of the active contour model may be expressed as shown below:

$$E_{snake} = \int_0^1 [\alpha(s)|\boldsymbol{v}'(s)|^2 + \beta(s)|\boldsymbol{v}''(s)|^2 - \gamma(s)|\nabla(G_\sigma(x,y) * I(x,y))|^2]ds \quad (1)$$

Where the former two integral items represents internal energy; the first derivative represents elastic energy and restrains the continuity of the curve; the second derivative represents bending energy and restrains the smoothness of the curve; and the third item represents external energy and leads the curve to approach the object. In order to extract the contour, the external energy restrains the curve reaching minimum at the image edges, and the gradient images are used for the expression. In the gradient images, ∇ signifies gradient operator, $G_\sigma * I$ signifies the convolution of Image I and the Gaussian smoothing filter with the standard deviation being σ. The purpose of the convolution is to reduce the influence of noise on the results. $\alpha(s)$、$\beta(s)$ and $\gamma(s)$ represent the various control weighing coefficients. The total curve energy expressed in Formula (1) within the whole image domain reaches the minimum pursuant to the variation principle, and the curve in conformity with conditions is the final result.

During the actual computing process Formula (1) must be discretized. Supposing that there are n points on the curve, i.e. $\boldsymbol{v}_i = (x_i, y_i)(i = 1, 2, ..., n)$, the first integral item in Formula (1) may be

discretized as $\alpha(i)\|\boldsymbol{v}_i-\boldsymbol{v}_{i-1}\|^2$, which is generally substituted with $(\bar{d}-\|\boldsymbol{v}_i-\boldsymbol{v}_{i-1}\|)^2$. Moreover, $\bar{d}$ signifies the mean distance between the points on the curve and its purpose is to ensure that the points on the curve distribute uniformly as distantly as possible. The second item may be discretized as $\beta(i)\|\boldsymbol{v}_{i+1}-2\boldsymbol{v}_i+\boldsymbol{v}_{i-1}\|^2$ and the third item may be discretized as $\gamma(i)E_{img}(i)$, where $E_{img}(i)$ signifies the value computed based on convolution and gradient at Point I. Finally, Formula (1) may be discretized as shown below:

$$E_{total}=\sum_{i=1}^{n}\alpha(i)(\bar{d}-\|\boldsymbol{v}_i-\boldsymbol{v}_{i-1}\|)^2+\beta(i)\|\boldsymbol{v}_{i+1}-2\boldsymbol{v}_i+\boldsymbol{v}_{i-1}\|^2-\gamma(i)E_{img}(i) \quad (2)$$

3. Improvement of active contour model

3.1. Image gravitation potential energy based on object-background gray value

3.1.1. Design of image gravitation potential energy

In regard to traditional models, the gradient force is a short-range force. When the initial vector data is located at a significant distance from the actual contour, the model may converge to local minimum so that it becomes impossible to obtain the true contour and the speed is very slow. Therefore, this paper designs a long-range force based on adequate prior information of the vector data. As shown in Figure 1, if the image is divided into two areas, namely the object and the background, their respective average gray values are Avg_o, Avg_b, their standard deviations are Std_o, Std_b, where O represents the center of the contour shape of the vector data, a,b respectively represent the points on the contour line of the vector data, and r_a, r_b represent the straight-line distances from a,b and O.

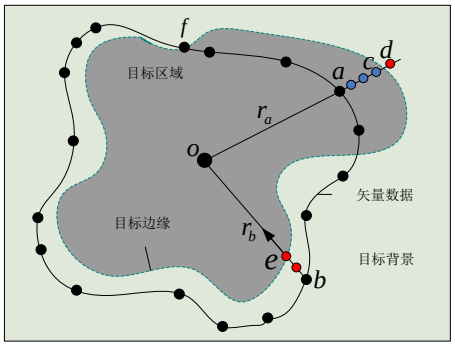

Figure 1. Image gravitation potential energy

Supposing that the image gravitation potential energy based on the object-background gray value is $E_{out}(i)$ at Point $\boldsymbol{v}_i$ and $E_{out}(i)$ represents the distance energy related to r_i, i.e. the distance between v_i and Point O, this potential energy must possess following function: when the points are located at a significant distance from the object's edges, rapidly pull the control points to approach to the true contour. Consequently, the $E_{out}(i)$ may be expressed with Formula (3):

$$E_{out}(i) = \mathrm{sgn}(i) / r_i^2 \qquad (3)$$

where $\mathrm{sgn}(i)$ is a sign function. If $\boldsymbol{v}_i$ is located within the area and $\mathrm{sgn}(i) = 1$, then r_i will increase during the energy minimization, $E_{out}(i)$ will decrease, and $\boldsymbol{v}_i$ will be forced to move outward, in a manner similar to Point a in Figure 1; on the contrary, if $\boldsymbol{v}_i$ is located outside of the area and $\mathrm{sgn}(i) = -1$, then both r_i and $E_{out}(i)$ will decrease during the energy minimization, and $\boldsymbol{v}_i$ will be forced to move inward, similar to Point b in Figure 1; when the points are close to the edges, $E_{out}(i)$ may be ineffective and $\mathrm{sgn}(i) = 0$, similar to Point f in Figure 1. During the minimization process, the points which are located far from edges, i.e. Points a, b, may be evolved toward edges at a certain step length along the r_a, r_b directions. Such a tactic produces a convergence speed which is faster than the evolution in the 3×3 or 5×5 ranges of the point. If the points oscillate around the edges (as Points c, d in Figure 1 do), then the evolution of the point will immediately cease, and the average location between the two oscillation points may be regarded as the final location of the point.

3.1.2. Automatic identification of object-background points based on range statistics

The key point of computing $E_{out}(i)$ is to determine where Point $\boldsymbol{v}_i$ is located, in the target area, either outside of the target area or at the edges. Therefore, the prior information of the area enclosed by the vector contour must be utilized adequately, i.e. the quantity proportion of the pixel points in the target area enclosed by the vector contour side line must be larger than those in the more distant background area; furthermore, the distribution of the pixel gray value in the target area must be more uniform than that in the background area, i.e. $Std_o < Std_b$; and finally, in regard to the water body, the mean gray value of the target area must be smaller than that of the background area farther, i.e. $Avg_o < Avg_b$. Based on the aforementioned prior information, this paper lists the steps of automatically determining the location area of $\boldsymbol{v}_i$, as described below:

① Compute the quantity of pixel points n in the area enclosed by the initial vector contour side line and count the pixel quantity n_q corresponding to every gray level q in [0,1...,255];

② Sort n_q in descending order, analyze the ranked n_q sequence $n_0, n_1, ..., n_t, ..., n_{255}$, and compute the n_t and corresponding gray level t. The t may be computed in the following manner: in the n_q sequence, $n_t - n_{t-1} > 10(n_{t-1} - n_{t-2})$, that is, the difference ratio of two adjacent sequences must be at least larger than a magnitude, and the t which conforms to such condition is the first t emerging in the ranked sequence. The purpose of this step is to identify and sum up the gray levels and pixel quantities of the target and the background areas enclosed by the vector data. In the ranked n_q sequence, $n_0, n_1, ..., n_t$ belong to the target area, and $n_{t+1}, n_{t+2}, ..., n_{255}$ belong to the background area.

③ Compute the mean pixel value Avg_o and standard deviation Std_o of the target area. Moreover,

$$Avg_o = \sum_{q=0}^{t} qn_q / \sum_{q=0}^{t} n_q \ , Std_o = \sqrt{\sum_{q=0}^{t} n_q (Avg_o - q) / \sum_{q=0}^{t} n_q} \ .$$

④ Identify the area where Point $\boldsymbol{v}_i$ is located. Supposing the mean gray value of the 3×3 or 5×5 range of Point $\boldsymbol{v}_i$ is avg, if $avg \le Avg_o + \lambda_1 Std_o$, then Point $\boldsymbol{v}_i$ is located in the area; if $avg > Avg_o + \lambda_2 Std_o$, then Point $\boldsymbol{v}_i$ is located outside of the area; if $Avg_o + \lambda_1 Std_o < avg \le Avg_o + \lambda_2 Std_o$, then Point $\boldsymbol{v}_i$ is located close to the area edges. According to the image quality, the value of λ_1 is generally between 1 and 2, and the value of λ_2 generally ranges between 4 and 6. In this paper, the value of λ_1 is 1 and that of λ_2 is 4.

3.2. Geometrical shape restriction based on similarity potential energy

When the traditional active contour model is used to extract the contour side line, the background noise will produce a strong attraction and disturbance to the contour side line, thus causing extraction failure. After comparing the vector data contour with the image contour, it was found that their respective contour shapes were roughly similar. In order to adequately utilize this prior information and reduce the influence of the noise, this paper introduces the similarity potential energy based on contour curvature.

Curvature is a parameter which may be used to describe the bending of a part of the curve; it also possesses displacement invariance and rotation

invariance, and has the characteristic of convex-concave invariance. Therefore, curvature is used to measure the similarity of the curve before and after evolution. As shown in Figure 2, the discrete curvature of Point $\boldsymbol{v}_i$, a point on the discrete curve, is $k_i = \mathrm{sgn}(i)\Delta\alpha_i / \Delta s_i$, where $\Delta\alpha_i$ signifies the angle between vectors $\boldsymbol{v}_{i-1}\boldsymbol{v}_i$ and $\boldsymbol{v}_i\boldsymbol{v}_{i+1}$, $\Delta s_i = \boldsymbol{v}_{i-1}\boldsymbol{v}_i + \boldsymbol{v}_i\boldsymbol{v}_{i+1}$ signifies the approximate arc length, and $\mathrm{sgn}(i)$ signifies the sign function. If Point $\boldsymbol{v}_i$ is convex, then $\mathrm{sgn}(i)$ is equal to 1; if it is concave, then $\mathrm{sgn}(i)$ is equal to -1.

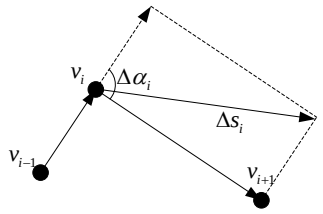

Figure 2. Discrete curvature

The similarity potential energy $E_{sim}(i)$ of Point $\boldsymbol{v}_i$ on the curve may be defined as follows:

$$E_{sim}(i) = (k_0(i) - k(i))^2 \qquad (4)$$

where $k_0(i)$ represents the curvature of Point $\boldsymbol{v}_i$ on the initial vector contour curve, and $k(i)$ represents the curvature of Point $\boldsymbol{v}_i$ on the current evolved contour curve.

Integrating Formulas (2), (3) and (4), the improved active contour model may be obtained:

$$E^*_{total} = \sum_{i=1}^{n} \alpha(i)(\bar{d} - \|\boldsymbol{v}_i - \boldsymbol{v}_{i-1}\|)^2 + \beta(i)\|\boldsymbol{v}_{i+1} - 2\boldsymbol{v}_i + \boldsymbol{v}_{i-1}\|^2 - \gamma(i)E_{img}(i) + \sigma(i)E_{out}(i) + \eta(i)E_{sim}(i) \qquad (5)$$

where $\sigma(i)$ and $\eta(i)$ represent the corresponding weight coefficients. It is possible to extract the extremals of the image edges after Formula (5) reaches the minimum within the whole image domain.

3.3. Solution and realization of the model

3.3.1. Design of image gravitation potential energy

There are many methods which may be used to solve the minimization of Formula (5), but the greedy algorithm presented by Amini (1990) and Williams (1992) is adopted most frequently. When using this algorithm, the convergence speed is high and the complexity is low. Although it is difficult to ensure global optimization, overall it is quite an effective method. This paper also utilizes the greedy algorithm to solve the model. The basic

principles of the greedy algorithm are as follows: in regard to any point $\boldsymbol{v}_i$ on the curve, as shown in Figure 3, first determine the Point $\boldsymbol{v}_{\min}$ which can minimize the Formula (5) in the neighborhood (3×3 is the neighborhood, as shown in the figure), then move Point $\boldsymbol{v}_i$ to Point $\boldsymbol{v}_{\min}$, and process $\boldsymbol{v}_1, \boldsymbol{v}_2, \ldots$ successively. After all points on the curve have been processed, an iteration may be formed and a new optimal curve may be generated.

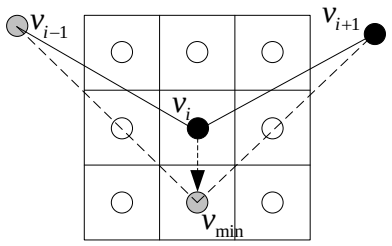

Figure 3. Search of optimal neighborhood of greedy algorithm

In order to improve the convergence speed and pull the vector data contour so that it approaches the edges rapidly, this paper proposes a two-stage processing tactic: In the first stage, the image gravitation plays the leading role and the rough contour of the object may be obtained. Moreover, in this stage the shape keeping is omitted. Thus, the $E_{out}(i)$ only reaches the minimum during the search based on the evolution plan shown in Section 3.1.1 In the second stage, the active contour model omits the $E_{out}(i)$ (i.e. omit the $E_{out}(i)$ in Formula (5)). This search tactic based on the greedy algorithm forces the rough contour to gradually approach the true one and ensures that the contour remains similar to the original shape.

During the second-stage search, the following tasks must be completed as well: ① Normalize all energy items listed in Formula (5). The normalization methods of the first and second items of internal and similarity potential energy $E_{sim}(i)$ must be the same, i.e. divide their maximums in the neighborhood then normalize the results to the intervals [0,1]. As for the third item $E_{img}(i)$, in order to highlight the effect of the gradient force, search the maximum $maxmag$ and minimum $minmag$ of each point on the curve in the neighborhood (supposing the gradient value of this point is mag), and normalize $E_{img}(i)$ using the formula $(minmag - mag)/(maxmag - minmag)$. If the gradient values in the neighborhood are similar, then the condition that $minmag = maxmag$ -5 if $maxmag$ - $minmag$ <5 may be made in order to avoid large deviation occurring to the gradient force. ② Self-adaptive increase and decrease of the quantity of points on the curve. In order to promote the edge refining ability of the model, a new point must be added in the center when the

distance between two points is larger than the set threshold (which is generally set as 0.2 mm). If the distance between two points is smaller than the set threshold, or three points are arranged in a straight line, then the corresponding points may be deleted. ③ Self-adaptive determination of weight coefficients. In most references, the weight coefficients $\alpha(i)$、$\beta(i)$、$\gamma(i)$ and $\eta(i)$ are set manually based on experience, and kept constant throughout the entire iterative process. The main issue with this method is that the coefficients may not be determined self-adaptively as the location and neighborhood of each point. In fact, when different points move around in their neighborhoods to search for the optimal value, the change rate of each energy item differs. If the same weight is applied to all points and different iterations, this will result in incorrect results. Consequently, this paper proposes a self-adaptive weight determination method: in regard to any point $\boldsymbol{v}_i$ on the curve, when it searches the optimal value in an $m \times m$ neighborhood, the model may record the energy values corresponding to each neighborhood point, then sum up and compute the standard deviations of those energy values. The reciprocals of each standard deviation are the weight coefficients of the energy items. The weight coefficients determined by this method may change self-adaptively according to the locations of the points on the curve.

3.3.2. Steps of the algorithm

Step 1: Register the vector data and remote sensing images precisely. Process the gray values of the images, unify and register the coordinate system and map projection of the remote sensing images and vector data, and build the mapping relationship between the image coordinates and geographic coordinates.

Step 2: Read the data of the vector contour side line of the area water body and initialize the model. Compute Avg_o and Std_o as shown in Section 3.1; compute $k_0(i)$ as shown in Section 3.2; compute the contour center of the vector side lines.

Step 3: First-stage search. Obtain the rough contour of the object as the search tactic as shown in Section 3.1.1, then stop searching.

Step 4: Begin second-stage search. Implement self-adaptive increase or decrease to the point quantity as described above in the section detailing the optimization tactic, so as to enhance the refining ability.

Step 5: Compute all points on the curve and move them to the locations with the minimum energies in the neighborhood, including the following specific steps:

① Count from i=1 to n (where n represents the quantity of the points on the initial vector curve) and compute the energy value $E_{snake,i}$ corresponding to Point i as shown in Formula (5) (after omitting $E_{out}(i)$).

② Count j=1 to m (where m represents the neighborhood pixel quantity of a single point on the curve. Here the 5×5 range is selected, i.e. m = 25). As for Point i on the curve, compute the respective values of $(\overline{d} - \|\boldsymbol{v}_j - \boldsymbol{v}_{j-1}\|)^2$ $\|\boldsymbol{v}_{j+1} - 2\boldsymbol{v}_j + \boldsymbol{v}_{j-1}\|^2$ $E_{img}(j)$ and $E_{sim}(j)$ of its neighborhood point, implement normalization in the neighborhood, compute the respective values of m energies, and sum up their standard deviations. The reciprocals of these standard deviations are the values of $\alpha(i)$、$\beta(i)$、$\gamma(i)$ and $\eta(i)$. This may be computed as follows:

$$E_j = \sum_{i=1}^{n} \alpha(i)(\overline{d} - \|\boldsymbol{v}_j - \boldsymbol{v}_{j-1}\|)^2 + \beta(i)\|\boldsymbol{v}_{j+1} - 2\boldsymbol{v}_j + \boldsymbol{v}_{j-1}\|^2 - \gamma(i)E_{img}(j) + \eta(i)E_{sim}(j)$$

If $E_j \le E_{snake,i}$ $E_{snake,i} = E_j$ and $j\min = j$. Meanwhile, the next j circulation may be performed until all j circulations are completed.

③ Move the No. i point $\boldsymbol{v}_i$ to the $\boldsymbol{v}_{j\min}$ location, i.e. $\boldsymbol{v}_i = \boldsymbol{v}_{j\min}$. Process the next point $\boldsymbol{v}_{i+1}$ until all i circulations have been completed.

The above circulation is the energy minimization process. The energy minimal points are searched for within the neighborhood range of each point on the curve during every circulation so as to substitute the original points.

Step 6: Sum up the moved point quantity in the second-stage optimization process, i.e. the quantity of the points which have locations with minimum energies differing from the original ones.

Step 7: When the quantity of the moved points remains the same or the total energy value fluctuates periodically, the computing shall be ceased immediately, otherwise, continue to Step 8. An iteration optimization in the second stage is completed during Steps 4- 7.

Step 8: Repeat Steps 4-7.

4. Precision evaluating model based on similarity measurement

In order to evaluate the performance and extracting precision of the model, the evaluating model is built based on the similarity measurements, and its basic goal is to measure the similarity between the extracted and true contour curves in the image. The true contour curve may be extracted manually. This paper makes measurements based on the shape similarity, neighboring degree of spatial location and area similarity. The contour side

lines extracted using the active contour model are expressed as the set of ordered points $A=\{P_i=(x_i,y_i)\,|\,i=1,2,...,N\}$, and the true contour curve extracted manually is expressed as $B=\{V_i=(x_i,y_i)\,|\,i=1,2,...,M\}$.

(1) Shape similarity: first, describe the contour side lines with center distance function. In regard to shape A (B similar), $S(P_i)$ signifies the distance between P_i and the center of contour shape A, thus allowing N values of $S(P_i)$ on the contour side line to be obtained. Normalize the mean value of $S(P_i)$, then implement the Fourier transform to the N $S(P_i)$, as shown below:

$$s(m)=\frac{1}{N}\sum_{i=0}^{N-1}S(P_i)\exp(\frac{-j2\pi mi}{N}),m=0,1,...,N-1 \qquad (6)$$

Obtain the coefficient vector $\boldsymbol{S}_A=[s(1),s(2),...,s(L)]$ via the former L coefficients after the Fourier transform. In general, the value of L is 16. If L is too large, the high frequency coefficients of the Fourier transform may contain noise. In the same manner, it is possible to obtain the $\boldsymbol{S}_B$ corresponding to the contour shape B. The similarity of shapes A and B may be expressed as shown below:

$$s_1=1-\|\boldsymbol{S}_A-\boldsymbol{S}_B\|\,(s_1\in[0,1]) \qquad (7)$$

(2) Neighboring degree of spatial location: The Hausdorff distance is applied to measure the neighboring degree of the locations (for the detailed computing process. refer to Sébastien (2008)). Supposing after normalization the Hausdorff distance between A and B is $H_{A,B}$, the neighboring degree of the location may be expressed as follows:

$$s_2=1-H_{A,B}(s_2\in[0,1]) \qquad (8)$$

(3) Area similarity: Supposing A_1 is the area of A and B_1 is the area of B, the area similarity may be expressed as follows:

$$s_3=1-|A_1-A_2|/\max(A_1,A_2)(s_3\in[0,1]) \qquad (9)$$

The computing formula of the total similarity $sim(A,B)$ may be obtained after integrating Formulas (7), (8) and (9), as shown below:

$$sim(A,B)=\omega_1 s_1+\omega_2 s_2+\omega_3 s_3 \qquad (10)$$

Where $\omega_1, \omega_2, \omega_3$ are corresponding weight coefficients, and in this paper their values are all 1/3. Thus, the result precision may be measured via $sim(A, B)$.

5. Experiment and analysis

5.1. Experimental area and data

The experimental area is located in an area of Suzhou region which contains dense waters. Three perennial lakes, namely H_1, H_2, H_3, were selected for use in the experiment. The vector data is the 1:1000000 data produced in the 1990s; the coordinate system is the 54 coordinate system; the projection is the conic orthermorphic projection; the currency of the image data is December 2010; and the image data is corrected orthophotos. The coordinate system is the WGS84 coordinate system and the projection is Mercator projection with a resolution of 10 m in both the horizontal and longitudinal directions, with a longitude range of 120°~121°30′ and latitude range of 30°~31°. The total image size is 14485×11391 pixels.

5.2. Experimental results and analysis

5.2.1. Experimental results

First the gray values of the image data were processed, and then converted from the WGS84 coordinate system to the 54 coordinate system, and from Mercator to conic orthermorphic projection. The vectors were overlaid with images, and the contour side lines of the lakes were extracted and updated as described in the realization steps shown in Section 3.3. Figures 4, 5 and 6 show the respective results of H_1, H_2, H_3. N represents the iterations in the second stage:

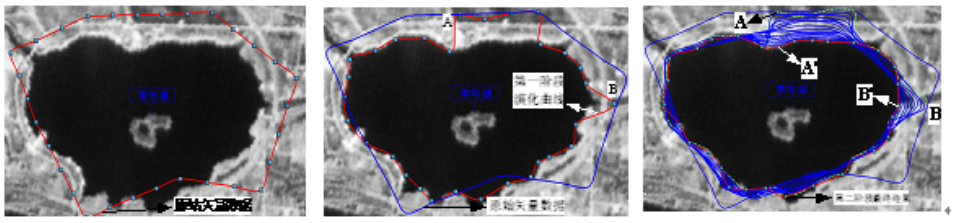

Avg_e=21.3， Std_e=19.7, s_1=0.86， s_1=0.90， s_2=0.88， s_3=0.94， N=16， s_1=0.97， s_2=0.96，
s_2=0.86， s_3=0.72， $sim(A, B)$=0.81 $sim(A, B)$=0.90 s_3=0.95 $sim(A, B)$=0.96

(a) Initial data (b) Results in first stage (c) Results in second stage

Figure 4. Experimental results of H_1

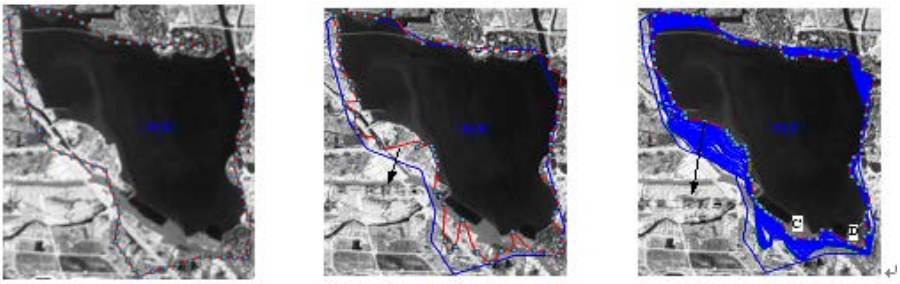

Avg_e=30.2， Std_e=20， s_1=0.71， s_2=0.84， s_3=0.77， $sim(A,B)$=0.77

s_1=0.79， s_2=0.89， s_3=0.88， $sim(A,B)$=0.84

N=38， s_1=0.92， s_2=0.93， s_3=0.99， $sim(A,B)$=0.95

(a) Initial data (b) Results in first stage (c) Results in second stage

Figure 5 Experimental results of H_2

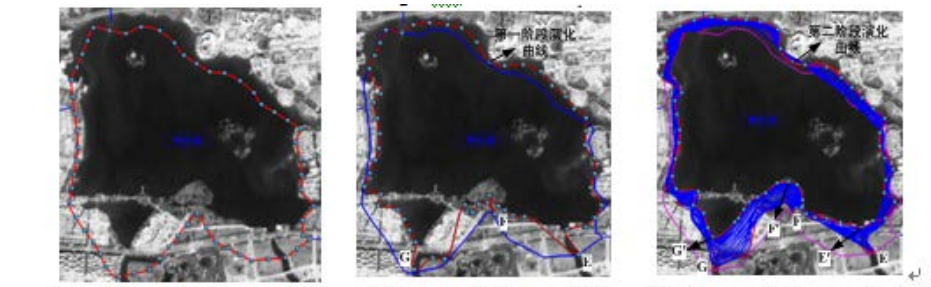

Avg_e=32， Std_e=12， s_1=0.90， s_2=0.70， s_3=0.88， $sim(A,B)$=0.83

s_1=0.9， s_2=0.89， s_3=0.98， $sim(A,B)$=0.91

N=22， s_1=0.96， s_2=0.93， s_3=0.96， $sim(A,B)$=0.95

(a) Initial data (b) Results in first stage (c) Results in second stage

Figure 6 .Experimental results of H_3

The graph of precisions corresponding to H_1 changing with iterations was then drawn, and is shown in Figure 7 (in a manner similar to H_2 and H_3):

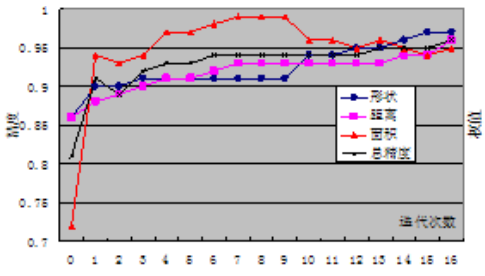

Figure 7. Relationships between precision and iterations

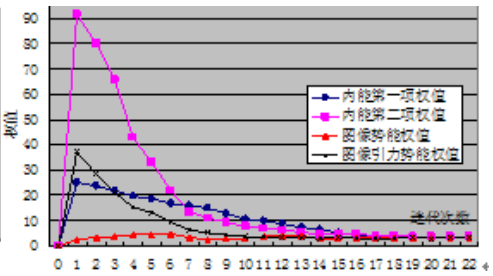

Figure 8. Relationships between weight and iterations

In order to analyze the weight changes occurring with the iterations, this paper analyzes the weight changes of Points E $\alpha(i)$、$\beta(i)$、$\gamma(i)$ and $\eta(i)$ in Figure 6 as they occur with the iterations, and the results are shown in Figure 8.

5.2.2. Analysis of boundary conditions of the results and model

After analyzing the results the following conclusions were drawn:

(1)After first-stage processing, most points on the vector contour curve approached the edges, and the extraction precision enhanced greatly compared with the initial vector data. However, due to the influence of noise points or surrounding rivers, the external background points may be mistakenly judged as the areas or edges, such as Points A, B, E, F and G shown in Figures 4, 5 and 6. These points cause the contour curve to differ greatly from the initial one.

(2)In the second stage, Points A, B, E, F and G, which previously reached local extreme points in the first stage, are forced to A′, B′, E′, F′ and G′, due to the effect of similarity restriction potential energy, and thus the final shape of the contour curve remains the same as the initial curve. In addition, in the second stage, the curve approaches the edges slowly, owing to the effect of short-range force and internal energy, and the precision enhances slowly; the model still possesses certain disadvantages over the extraction of the weak edges, such as Areas C and D, as shown in Figure 5 (c).

(3)It is clearly known from Figure 7 that the total extraction precision, neighboring degree of distance and shape similarity all increase slowly with the increase of iterations, while the area precision fluctuates. When the number of iterations are more than 10 times, the four precisions tend to gradually become consistent. This phenomenon conforms to the evolution law of the curve; it is known from Figure 8 that in the initial iterative stage the weight coefficients differ greatly. However, with the increase of iterations, the weights decrease gradually and tend to become consistent, which adequately indicates that the change rates of energy items are inconsistent at the beginning of iteration when the points move in the neighborhood, whereas when the iterations increase, the change rates tend to become consistent. It is therefore shown that when the weights are determined based on personal experiences, incorrect results may be produced.

Due to the fact that the active contour model is sensitive to initial location, further discussion regarding the initial boundary conditions of the model is made below:

(1)The area ratio between the area water body in the images enclosed by the vector data and vector data must be larger than 50%, otherwise the model may not be able identify the background and object points automatically, as described in the method detailed in Section 3.1.

(2)The vector contour must be very similar to the image contour in shape and the two contours must not differ greatly, otherwise the similarity restriction potential energy may exhibit a reaction.

The above two boundary conditions are absolutely necessary. However, the present model may not be able to detect the two boundary conditions automatically. Human-computer interaction with the area water body must be performed, resulting in poor extraction effect, due to the inconformity with the aforementioned two boundary conditions involved in the specific application process.

5.3. Algorithm comparison and analysis

The H_1 described in Section 5.1 is selected as the experimental datum to compare the differences in results and efficiency between the method discussed in this paper and the initial active contour model (the grouping snake model presented in Kass(1987) and HAN(2009)). Figures 9 (a) and (b) show the results obtained by means of the initial active contour model (the greedy algorithm is also adopted as a solving method) and the grouping snake model. Table 1 shows the comparison between extraction precision and consumed time:

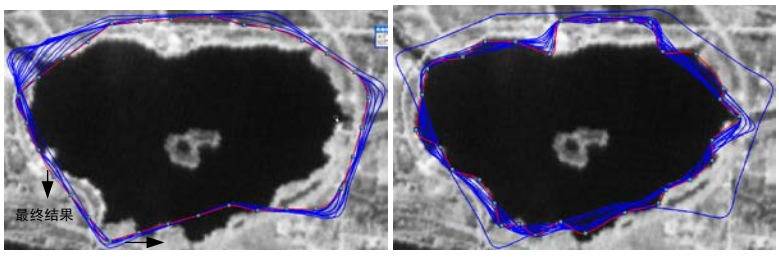

Figure 9 Extraction results of traditional model and Reference [7]

Extraction method	s_1	s_2	s_3	$sim(A, B)$	Consumed time
Kass(1987)	0.83	0.88	0.76	0.82	2.8s
HAN(2009)	0.90	0.88	0.92	0.90	4.9s
This paper	0.97	0.96	0.95	0.96	3.3s

Table 1. Comparison of extraction algorithm

After comparing the three methods the following conclusions were drawn:

(1)It is difficult for the traditional model to converge to the contour edges due to the limitations of noise influence and sphere of action of the gradient force, and thus the extraction precision is low.

(2)The grouping snake model shows a great improvement over the traditional methods, as it may converge to the contour edges in the area with no noise influence. If it is affected by noise, the points on the curve may converge to local extreme points easily, causing the process to require a large amount of time.

In summary, the method raised in this paper is a great improvement in noise immunity and extraction precision over the active contour model previously used.

6. Conclusion

Not only may the existing vector data be used as the initial location of the active contour model, but they may also provide a large amount of previously existing knowledge during the process of extracting and updating the area water body with the active contour model from the remote sensing image data. This paper adequately utilizes previously existing knowledge, adds similarity restriction potential energy (the purpose of which is to avoid the attraction and disturbance of noise points to the points on the contour curve and avoid large amounts of deformation from occurring between the final curve and actual results) and image gravitation potential energy (the purpose of which is to enhance the convergence speed of the model) based on the traditional active contour model; then the paper adopts a two-stage search tactic during model solving, solves the problem of self-adaptive determination of weight coefficients, and builds the precision evaluating model based on similarity measurement. Finally, the results of experiments show the feasibility and

superiority of the proposed method. The disadvantages and the aspects which require further study include the following:

(1) Further improve the model in order to make it available for the extraction of weak edges (i.e. Areas C and D in Figure 5 (c)).

(2)Settle the matching problem of the image and vector objects not being 1:1. The paper extracts and updates the area water body using the vector data and active contour model, with the one precondition that the vector and image objects must be 1:1. Only in this way may the vector data be used as the initial location of the active contour model. If there are vector data but no corresponding objects in the images (1:0), or if there are objects in the images but no vector data (0:1), then one vector datum corresponds to multiple image objects or multiple vector objects correspond to one image object (1:N or N:1), or multiple vector objects correspond to multiple image objects (M:N), and the issue which requires further study is how to determine and solve the aforementioned situations automatically.

References

Amini A, Weymouth T and Jain R(1990)Using dynamic programming for solving variational problems in vision. IEEE Transaction on Pattern Analysis and Machine Intelligence 12(9):855-867(14)

CHEN Bo, LAI Jianhuang(2007) Active Contour Models on Image Segmentation: A Survey . Journal of Image and Graphics 12(1):11-20[in Chinese](8)

CHEN Jun, WANG Donghua, ShANG Yaoling, et al (2010) Master Design and Technical Development for National 1:50000 Topographic Database Updating Engineering in China . Acta Geodaetica et Cartographica Sinica 39(1):7-10[in Chinese](10)

HAN Min, SUN Yang(2009)A Method of Vector Edge Updating Based on Grouping Snake Model in GIS. Acta Geodaetica et Cartographica Sinica 38(2):168-173[in Chinese](9)

HU Yang, ZU Keju(2009) Road Extraction from Remote Sensing Imagery Based on Road Tracking and Ribbon Snake. In: Pacific-Asia Conference on Knowledge Engineering and Software Engineering 201-204(5)

Kass M, Witkin A, Terzopoulos D(1987)Snakes： Active Contour Models, International Journal of Computer Vision 1(4)： 321—331(7)

Matthias Butenuth, Christian Heipke(2010)Network snakes: graph-based object delineation with active contour models. Machine Vision and Applications 21(8): 1207-1221(2)

Matthias Butenuth, Bernd-Michael Straub, and Christian Heipke(2004) Automatic Extraction of Field Boundaries from Aerial Imagery. In KDNet Symposium on Knowledge-Based Services for the Public Sector 14-25(3)

Matthias Butenuth(2007)Segmentation of imagery using network snakes. Photogram-metrie Fernerkundung Geoinformation 1: 7-16(4)

Matthias Butenuth, Guido v. Gösseln, Michael Tiedge, et al (2007) Integration of heterogeneous geospatial data in a federated database. ISPRS Journal of Photogrammetry & Remote Sensing 62:328-346(13)

MIAO Lixin, TANG Shouzheng, LI Xia, et al (2010) Extract reservoir water area automatically using masked active contour model from multi-spectral remote sensing images. Research of Soil and Water Conservation 17(5): 7-11[in Chinese](6)

SALMAN Ahmadi, M.J. Valadan Zoej, Hamid Ebadi, et al (2010) Automatic urban building boundary extraction from high resolution aerial images using an innovative model of active contours. International Journal of Applied Earth Observation and Geoinformation 12:150-157(1)

Sébastien Mustière, Thomas Devogele(2008) Matching Networks with Different Levels of Detail. Geoinformatica 12: 435 -453(16)

Stefan Hinz(2008) Automatic object extraction for change detection and GIS update. In: The International Archives of the Photogrammetry, Remote Sensing and Spatial Information Sciences Vol. XXXVII, Part B4: 277-284(12)

Williams DJ, Shah M (1992) A fast algorithm for active contours and curvature estimation. CVGIP: Image Understanding 55(1):14-26(15)

ZHANG Jianqing, ZHU Lina, PAN Li (2007) River Change Detection Based on Remote Sensing Imagery and Vector Data. Geomatics and Information Science of Wuhan University 32(8):663-666(11)